# Bicontinuous Microemulsions under Steady Shear Flow

Hiroya Kodama ([1,*]) and Shigeyuki Komura ([2])

([1]) Graduate School of Science and Technology, Kobe University, Kobe 657, Japan
([2]) Department of Mechanical System Engineering, Kyushu Institute of Technology, Iizuka 820, Japan

*(Received 30 August 1996, accepted 7 October 1996)*

PACS.64.75.+g – Solubility, segregation, and mixing; phase separation
PACS.68.10.Jy – Kinetics (evaporation, adsorption, condensation, catalysis, etc.)
PACS.82.20.Wt – Computational modeling; simulation

**Abstract.** — Dynamic response of microemulsions to shear deformation on the basis of two-order-parameter time dependent Ginzburg-Landau model is investigated by means of cell dynamical system approach. Time evolution of anisotropic factor and excess shear stress under steady shear flow is studied by changing shear rate and total amount of surfactant. As the surfactant concentration is increased, overshoot peak height of the anisotropic factor increases whereas that of the excess shear stress is almost unchanged.

## 1. Introduction

Microemulsions being mixture of oil, water and surfactant are known to exhibit various interesting mesoscopic structures depending on the temperature or the composition [1]. When the concentration of surfactant is relatively large, they show a rich variety of regularly ordered structures such as the cubic phase, the hexagonal phase or the lamellar phase. By lowering the concentration of surfactant and if the volumes of oil and water are not very different, microemulsions form a bicontinuous structure where a multiply connected randomly oriented monolayer of surfactants separate oil-rich and water-rich subvolumes with a mesoscopic length scale ($10 \sim 100$ nm).

When one quenches the ternary system from a high temperature homogeneous phase where the system is uniformly mixed to a low temperature phase where a certain structure exists, the average domain size increases in time until it reaches the equilibrium size. Several people have investigated such a dynamics of phase separation using different models. Kawakatsu *et al.* have proposed a "hybrid model" where oil and water are represented by coarse-grained fields and surfactants are treated microscopically [2], whereas Laradji *et al.* performed molecular dynamics simulations [3]. In the different paper by Laradji and his coworkers, a phenomenological two-order-parameter Ginzburg-Landau free energy has been proposed associated with standard time dependent Ginzburg-Landau (TDGL) equations [4]. In their model, one of the order parameters represents the local concentration difference between oil and water, while the other represents the local surfactant concentration. Recently, Pätzold and Dawson extended this study to incorporate the hydrodynamic effects by coupling the TDGL equations to Navier-Stokes-type equations [5]. All of these works have shown that systems containing

(*) Author for correspondence (e-mail: hkodama@icluna.kobe-u.ac.jp)

surfactants exhibit a slow non-algebraic growth of the domains, in contrast to the ordinary spinodal decomposition of pure binary systems.

Another aspect of the dynamics of microemulsions is related to the structural change in response to externally applied perturbations. The rheological properties of microemulsions have been theoretically investigated by Mundy *et al.* using a single-order-parameter TDGL model [6] and later extended by Pätzold and Dawson who also performed computer simulations [7]. Here the only order parameter describes the concentration difference between oil and water and the presence of surfactants is taken into account through surface tension parameter. (This point will be discussed later.) In reference [7], authors showed that the microemulsions behave in an essentially non-Newtonian manner.

As discussed in the paper by Pätzold and Dawson [7], the next step in the computational study of the rheology of microemulsions is to include the surfactant concentration field. Generally speaking, for a ternary mixture, it is natural to characterize the system in terms of two independent concentration variables. The aim of this paper is to investigate the dynamic response of microemulsions to shear deformation on the basis of two-order-parameter Ginzburg-Landau model. For this purpose, one may naturally think of employing the above mentioned Laradji's two-order-parameter model [4]. According to our preliminary numerical study of Laradji's model, however, we found that the domains do not flow globally even in the presence of the convective macroscopic flow. This problem seems to be related to the fact that Laradji's model is not well-defined, since the free energy of configurations with large surfactant concentration at the oil/water interfaces is not bounded from below as pointed out in the book by Gompper and Schick [1]. In fact, we observed the divergence of the surfactant concentration at the oil/water interfaces as we decreased the simulation mesh size.

## 2. Model

Here we use a different two-order-parameter free energy functional which has been proposed in our previous paper [8]. Our model is indeed bounded from below and has no drawbacks mentioned above. Let $\psi(\mathbf{r})$ describes the local concentration difference of oil and water, and $\rho(\mathbf{r})$ the local surfactant concentration. What we have required in our model is that (i) the profiles of $\psi$ and $\rho$ at the oil/water interfaces do not depend on the average values of $\psi$ and $\rho$ (denoted hereafter as $\overline{\psi}$ and $\overline{\rho}$, respectively) and (ii) the coarse-graining dynamics of $\psi$ based on the free energy becomes slow when the amplitude of $\rho$ at the interfaces takes a certain saturated value. The minimum model which fulfils these requirements is [8]

$$F = \int \mathrm{d}\mathbf{r} \left[ w(\nabla^2\psi)^2 + d(\nabla\psi)^2 - a\psi^2 + u\psi^4 + e\rho^2(\rho - \rho_\mathrm{s})^2 - s\rho(\nabla\psi)^2 \right], \tag{1}$$

where $w$, $d$, $a$, $u$, $e$, $\rho_\mathrm{s}$ and $s$ are positive constants. The last term $-s\rho(\nabla\psi)^2$ favors the surfactants to sit at the oil/water interfaces [4]. The double-minimum potential $e\rho^2(\rho - \rho_\mathrm{s})^2$ guarantees that $\rho$ locally takes the value either 0 or $\rho_\mathrm{s}$, whereas positive $w$ prevents the model from becoming unbounded.

For the time evolution of $\psi(\mathbf{r}, t)$ and $\rho(\mathbf{r}, t)$, we assume the standard TDGL equations. Both $\psi$ and $\rho$ are conserved quantities. Since we consider the case that there is a macroscopic flow $\mathbf{v}$, TDGL equations acquire a convective term and become

$$\frac{\partial\psi}{\partial t} + \nabla\cdot(\mathbf{v}\psi) = M_\psi\nabla^2\frac{\delta F}{\delta\psi} + \eta_\psi(\mathbf{r}, t), \tag{2}$$

$$\frac{\partial\rho}{\partial t} + \nabla\cdot(\mathbf{v}\rho) = M_\rho\nabla^2\frac{\delta F}{\delta\rho} + \eta_\rho(\mathbf{r}, t). \tag{3}$$

Here $M_\psi$ and $M_\rho$ are transport coefficients, and $\eta_\psi$ and $\eta_\rho$ represent thermal noise which satisfy the fluctuation-dissipation theorem

$$\langle \eta_{\psi(\rho)}(\mathbf{r},t)\eta_{\psi(\rho)}(\mathbf{r}',t')\rangle = -2k_{\mathrm{B}}TM_{\psi(\rho)}\nabla^2\delta(\mathbf{r}-\mathbf{r}')\delta(t-t'), \tag{4}$$

where $k_{\mathrm{B}}$ is the Boltzmann constant and $T$ is the temperature. As regards the macroscopic flow in equations (2) and (3), we consider a simple shear flow $v_x(\mathbf{r}) = \dot{\gamma}y, v_y = v_z = 0$, where the shear rate $\dot{\gamma}$ is the time derivative of the strain $\gamma$. By inserting equation (1) into equations (2) and (3), the time evolution equations can be explicitly written as

$$\frac{\partial\psi}{\partial t} = -\dot{\gamma}y\frac{\partial\psi}{\partial x} + M_\psi\nabla^2\left[-2a\psi + 4u\psi^3 + 2w\nabla^4\psi - 2(d-s\rho)\nabla^2\psi + 2s(\nabla\psi)\cdot(\nabla\rho)\right] + \eta_\psi(\mathbf{r},t), \tag{5}$$

$$\frac{\partial\rho}{\partial t} = -\dot{\gamma}y\frac{\partial\rho}{\partial x} + M_\rho\nabla^2\left[2e\rho(\rho-\rho_{\mathrm{s}})(2\rho-\rho_{\mathrm{s}}) - s(\nabla\psi)^2\right] + \eta_\rho(\mathbf{r},t). \tag{6}$$

In our work, we have entirely ignored the hydrodynamic interactions which might play an important role in microemulsions.

## 3. Cell Dynamical System Approach

In order to solve the above time evolution equations, we used the cell dynamical system (CDS) approach proposed by Oono *et al.* [9]. The CDS model is a space-time discrete model to describe a phenomena at the mesoscopic level and proved to be an efficient algorithm for numerical simulations. Here we restricted ourselves to a two-dimensional system. Accordingly, the space coordinate is specified by the lattice point $\mathbf{n} = (n_x, n_y)$ in an $L \times L$ square lattice. The CDS equations corresponding to equations (5) and (6) are

$$\psi(\mathbf{n},t+1) = \psi(\mathbf{n},t) - \dot{\gamma}n_y\tilde{\partial}_x\psi(\mathbf{n},t) + M_\psi\tilde{\nabla}^2\mathcal{I}(\mathbf{n},t) + C_\psi\eta(\mathbf{n},t), \tag{7}$$

$$\rho(\mathbf{n},t+1) = \rho(\mathbf{n},t) - \dot{\gamma}n_y\tilde{\partial}_x\rho(\mathbf{n},t) + M_\rho\tilde{\nabla}^2\mathcal{J}(\mathbf{n},t) + C_\rho\eta'(\mathbf{n},t), \tag{8}$$

where $\mathcal{I}(\mathbf{n},t)$ and $\mathcal{J}(\mathbf{n},t)$ are the discrete thermodynamic forces given by

$$\mathcal{I}(\mathbf{n},t) = -A\tanh\psi + \psi + W(\tilde{\nabla}^2)^2\psi - (D-S\rho)\tilde{\nabla}^2\psi + S(\tilde{\nabla}\psi)\cdot(\tilde{\nabla}\rho), \tag{9}$$

$$\mathcal{J}(\mathbf{n},t) = E\rho(\rho-\rho_{\mathrm{s}})(2\rho-\rho_{\mathrm{s}}) - \frac{1}{2}S(\tilde{\nabla}\psi)^2, \tag{10}$$

respectively. The "tanh" term in equation (9) is introduced for the sake of numerical stability [9]. In the above equations, the discretized differential operators are defined as

$$\tilde{\nabla}\phi = (\tilde{\partial}_x\phi, \tilde{\partial}_y\phi) = \frac{1}{2}\big(\phi(n_x+1,n_y) - \phi(n_x-1,n_y), \phi(n_x,n_y+1) - \phi(n_x,n_y-1)\big) \tag{11}$$

and

$$\tilde{\nabla}^2\phi = \frac{1}{2}\sum\phi(\text{nearest-neighbor cells}) + \frac{1}{4}\sum\phi(\text{next-nearest-neighbor cells}) - 3\phi. \tag{12}$$

($\phi$ denotes either $\psi$ or $\rho$.) The noise terms in equations (7) and (8) are given by

$$\eta^{(\prime)}(\mathbf{n},t) = \eta_x^{(\prime)}(n_x+1,n_y,t) - \eta_x^{(\prime)}(n_x,n_y,t) + \eta_y^{(\prime)}(n_x,n_y+1,t) - \eta_y^{(\prime)}(n_x,n_y,t), \tag{13}$$

where $\eta_x^{(\prime)}$ and $\eta_y^{(\prime)}$ are random numbers uniformly distributed in the interval $[-1,1]$ and $C_{\psi(\rho)}$ are the noise amplitudes taken as independent parameters in CDS [10]. In the presence of

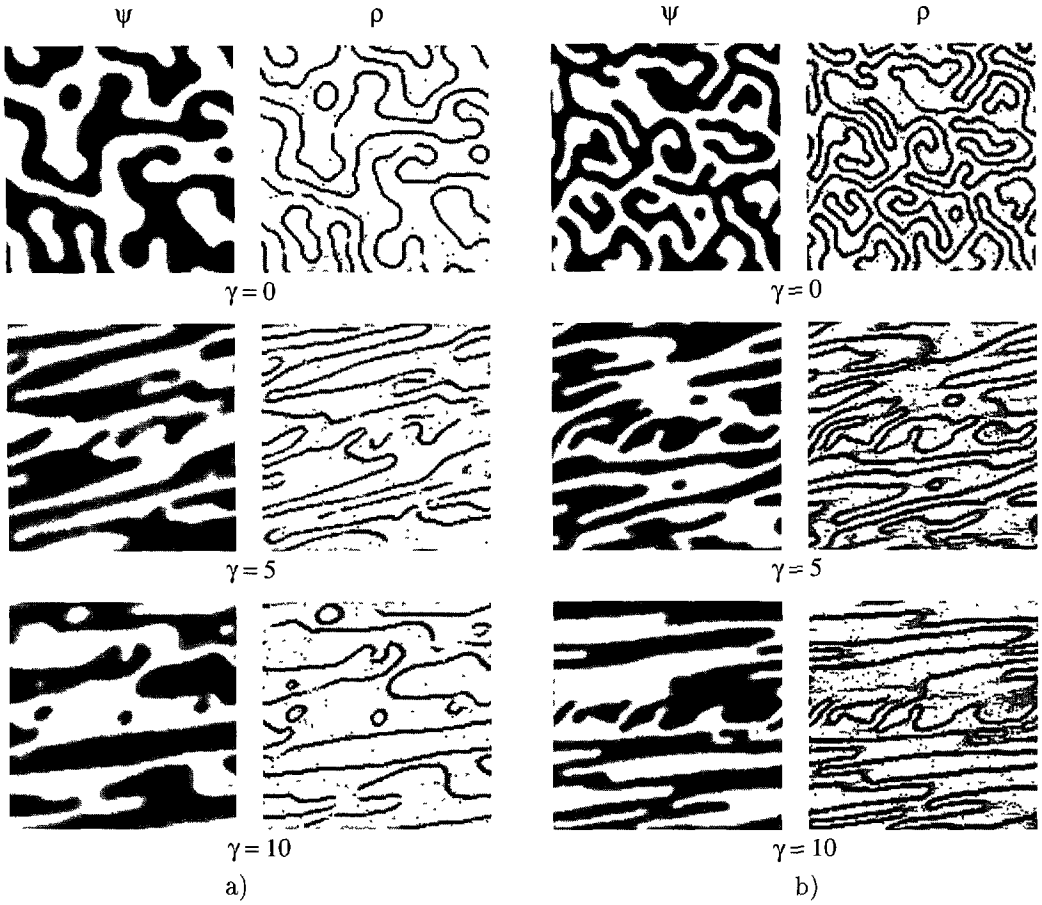


Fig. 1. — Time evolution of $\psi$ (left) and $\rho$ (right) for (a) $\overline{\rho} = 0.1$, $\dot{\gamma} = 2 \times 10^{-4}$, (b) $\overline{\rho} = 0.4$, $\dot{\gamma} = 2 \times 10^{-4}$, (c) $\overline{\rho} = 0.1$, $\dot{\gamma} = 2 \times 10^{-3}$ and (d) $\overline{\rho} = 0.4$, $\dot{\gamma} = 2 \times 10^{-3}$ every 5 strains.

the shear flow, we required a boundary condition such that

$$\phi(n_x, n_y, t) = \phi(n_x + \imath L + \gamma j L, n_y + jL, t) \tag{14}$$

holds for arbitrary integers $i$ and $j$ [11]. The initial distributions of $\psi$ and $\rho$ are specified by a random uniform distribution in the range $[\overline{\psi} - 0.01, \overline{\psi} + 0.01]$ and $[\overline{\rho} - 0.01, \overline{\rho} + 0.01]$, respectively. In our simulations, we fixed the parameters as $L = 128$, $A = 1.3$, $W = 0.2$, $D = 0.5$, $S = 0.5$, $E = 0.25$, $\rho_s = 1$, $M_\psi = M_\rho = 0.05$, $C_\psi = C_\rho = 0.02$ and $\overline{\psi} = 0$, whereas $\overline{\rho}$ has been changed as $\overline{\rho} = 0.1, 0.2, 0.3$ and 0.4. Notice that our parameter choice satisfies $D = S\rho_s$ which ensures the interfacial tension to vanish when $\rho = \rho_s$. Before the shear flow is applied, equations (7) and (8) are numerically solved up to $5 \times 10^5$ time steps. The average domain size in the equilibrium pattern of $\psi$ decreases when $\overline{\rho}$ is increased as has been observed experimentally [12] and theoretically [4, 13]. The scaling behavior to reach the equilibrium configurations within our model has been analyzed previously [8]. Hereafter the time origin is taken as the instance when the shear flow is turned on. The application of the steady shear flow is tried for $\dot{\gamma} = 2 \times 10^{-4}$, $5 \times 10^{-4}$, $1 \times 10^{-3}$ and $2 \times 10^{-3}$

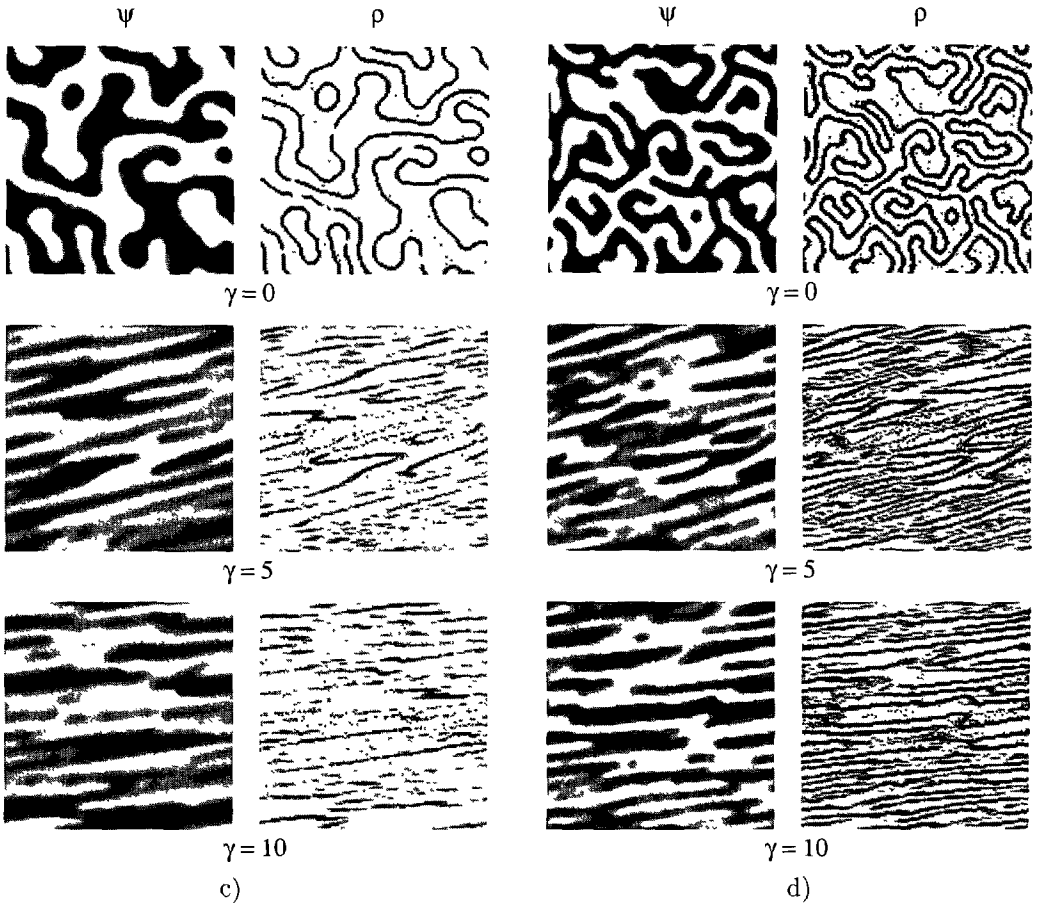


Fig. 1. — *(Continued.)*

## 4. Results and Discussions

Typical time evolutions of $\psi$ and $\rho$ are shown in Figure 1 for (a) $\overline{\rho} = 0.1$, $\dot{\gamma} = 2 \times 10^{-4}$, (b) $\overline{\rho} = 0.4$, $\dot{\gamma} = 2 \times 10^{-4}$, (c) $\overline{\rho} = 0.1$, $\dot{\gamma} = 2 \times 10^{-3}$ and (d) $\overline{\rho} = 0.4$, $\dot{\gamma} = 2 \times 10^{-3}$. By changing $\overline{\rho}$ and $\dot{\gamma}$, we found the following general behaviors. When the shear rate is small (Figs. 1a, b), surfactants move under the flow keeping themselves attached to the oil/water interfaces. The total amount of the interface does not seem to change appreciably during the deformation. On the other hand, when the shear rate is large (Figs. 1c, d), the surfactants cannot saturate all the interfaces. The coagulation and break-up processes take place as has been observed in the spinodal decomposition under steady shear flow [11] and the total amount of the interface increases.

Given the evolving patterns, we have evaluated the anisotropic factor defined by [6,7]

$$Q_{xy} = \frac{1}{\Omega} \sum_{\mathbf{n}} \left[ -D(\tilde{\partial}_x \psi)(\tilde{\partial}_y \psi) - 2W(\tilde{\partial}_x \tilde{\partial}_y \psi)(\tilde{\nabla}^2 \psi) \right], \tag{15}$$

where $\Omega$ is the total volume (area) of the system. Although this quantity essentially represents the $xy$-component of the macroscopic excess stress tensor in the case of spinodal decomposition

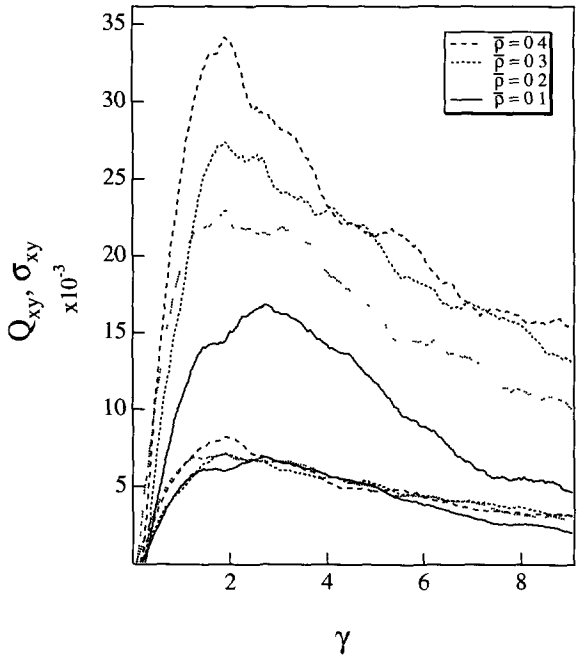


Fig. 2. — The anisotropic factor $Q_{xy}$ (upper 4 curves, see Eq. (15)) and the shear stress $\sigma_{xy}$ (lower 4 curves, see Eq. (16)) as a function of the shear strain $\gamma = \dot{\gamma}t$ for fixed $\dot{\gamma} = 2 \times 10^{-4}$ and $\overline{\rho} = 0.1$, 0.2, 0.3, 0.4.

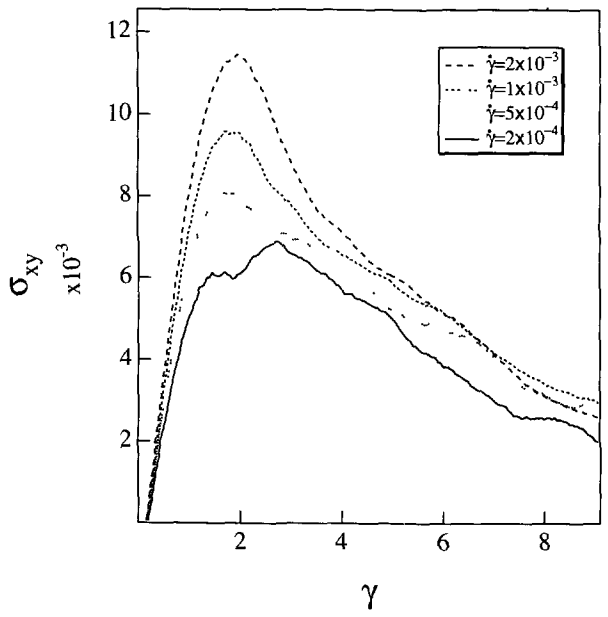


Fig. 3. — The shear stress $\sigma_{xy}$ (see Eq. (16)) as a function of the shear strain $\gamma = \dot{\gamma}t$ for fixed $\overline{\rho} = 0.1$ and $\dot{\gamma} = 2 \times 10^{-4}$, $5 \times 10^{-4}$, $1 \times 10^{-3}$, $2 \times 10^{-3}$ from bottom to top.

without any surfactants [11], this is not the case in the present model since there should be a contribution to the stress due to the non-local coupling term in equation (1). Nevertheless the problem of stress division between $\psi$ and $\rho$ is theoretically not yet clear. Instead, we propose here the following quantity

$$\sigma_{xy} = \frac{1}{\Omega} \sum_{\mathbf{n}} \left[ -(D - S\rho)(\tilde{\partial}_x \psi)(\tilde{\partial}_y \psi) - 2W(\tilde{\partial}_x \tilde{\partial}_y \psi)(\tilde{\nabla}^2 \psi) \right], \tag{16}$$

which is assumed to express the excess shear stress. Figure 2 shows the plot of $Q_{xy}$ and $\sigma_{xy}$ as a function of the shear strain $\gamma$ for several values of $\overline{\rho}$. Here the shear rate is fixed as $\dot{\gamma} = 2 \times 10^{-4}$ In Figure 3, we also plotted $\sigma_{xy}$ for several values of $\dot{\gamma}$ fixing the total amount of surfactants as $\overline{\rho} = 0.1$. It is seen that both $Q_{xy}$ and $\sigma_{xy}$ initially increase rapidly and then decrease. We observed that the strain giving the peak position of $Q_{xy}$ and $\sigma_{xy}$ is almost constant, $\gamma_{\text{peak}} \approx 2$, through the present simulation. On the other hand, the peak height of $Q_{xy}$ is larger than that of $\sigma_{xy}$ as a whole. $\overline{\rho}$ dependencies of the peak height of $Q_{xy}$ and $\sigma_{xy}$ are also different; the peak height of $Q_{xy}$ increases linearly with $\overline{\rho}$, while that of $\sigma_{xy}$ is almost independent of $\overline{\rho}$. However, a clear shear rate dependence of the peak height of $\sigma_{xy}$ is observed in Figure 3 as in reference [11].

Finally we comment on the difference between the present rheological study based on the two-order-parameter model and the previous works [6, 7] which essentially utilize the single-order-parameter free energy proposed by Teubner and Strey to describe the microemulsion phase [14]

$$F_{\text{TS}} = \int \mathrm{d}\mathbf{r} \left[ \mathcal{A}(\nabla^2 \psi)^2 - \mathcal{B}(\nabla \psi)^2 + \mathcal{C}\psi^2 \right], \tag{17}$$

where $\mathcal{A}, \mathcal{B}$ and $\mathcal{C}$ are positive constants ($\mathcal{B}$ is the surface tension parameter). This free energy is consistent with the observed scattering function which shows a peak at non-zero wavevector $q$ and falls off as $q^{-4}$ at large wavevectors [14]. Since $\mathcal{C} > 0$ in equation (17), $\psi$ locally prefers to vanish, $\psi \approx 0$, whereas $\psi$ takes either $\psi \approx \pm\sqrt{a/2u} \neq 0$ for equation (1). (Notice that $a$ in Eq. (1) is defined as positive.) In this sense, previous rheological studies of microemulsions [6, 7] have examined essentially the disordered phase as in the study of the rheology of block copolymer melts near to the critical point [15]. In our work, on the other hand, we observe motions of domains with sharp oil/water interfaces, and hence dealing with dynamics of ordered phase. Similar approaches to the phase separating binary mixture [11] or the ordered block copolymers [16] have been also reported.

In summary, within the CDS approach, we have investigated the effect of the steady shear flow on bicontinuous microemulsions by changing the average surfactant concentration and the shear rate. Details of our results will be published elsewhere that will also include the case where the concentrations of water and oil are different from each other.

## Acknowledgments

We would like to thank Prof. Shigehiro Komura and Dr. J.L. Harden for their helpful discussions. This work is supported by the Ministry of Education, Science and Culture, Japan (Grant-in-Aid for Scientific Research No. 08226233, No. 08740324 and No. 0657).

## References


[1] Gompper G. and Schick M., Self-Assembling Amphiphilic Systems (Academic Press, 1994).

[2] Kawasaki K. and Kawakatsu K., *Physica A* **164** (1990) 549; Kawakatsu K. and Kawasaki K., *ibid.* **167** (1990) 690.

[3] Laradji M., Mouristen O.G., Toxvaerd S. and Zuckermann M.J., *Phys. Rev. E* **50** (1994) 1243.

[4] Laradji M., Guo H., Grant M. and Zuckermann M.J., *J. Phys. A* **24** (1991) L629; *J. Phys. Condens. Matter* **4** (1992) 6715.

[5] Pätzold G. and Dawson K., *Phys. Rev. E* **52** (1995) 6908.

[6] Mundy C.J., Levin Y. and Dawson K.A., *J. Chem. Phys.* **97** (1992) 7695.

[7] Pätzold G. and Dawson K., *J. Chem. Phys.* **104** (1996) 5932.

[8] Komura S. and Kodama H., submitted.

[9] Oono Y. and Puri S., *Phys. Rev. Lett.* **58** (1987) 836; *Phys. Rev. A* **38** (1988) 434.

[10] Puri S. and Oono Y., *J. Phys. A* **21** (1988) L.755.

[11] Ohta T., Nozaki H. and Doi M., *Phys. Lett. A* **145** (1990) 304; *J. Chem. Phys.* **93** (1990) 2664.

[12] Kotlarchyk M., Chen S.-H., Huang J.S. and Kim M.W., *Phys. Rev. Lett.* **53** (1984) 941.

[13] Laradji M., Guo H., Grant M. and Zuckermann M.J., *Phys. Rev. A* **44** (1988) 8184.

[14] Teubner M. and Strey R., *J. Chem. Phys.* **87** (1987) 3195.

[15] Fredrickson G. and Larson R.G., *J. Chem. Phys.* **86** (1987) 1553; Onuki A., *J. Chem. Phys.* **87** (1987) 3692.

[16] Ohta T., Enomoto Y., Harden J.H. and Doi M., *Macromolecules* **26** (1993) 4928; Kodama H. and Doi M., *Macromolecules* **29** (1996) 2652.